Swiss J Geosci (2010) 103:535–549
DOI 10.1007/s00015-010-0039-8

Earthquakes in Switzerland and surrounding regions during 2009

Nicholas Deichmann · John Clinton · Stephan Husen · Benjamin Edwards · Florian Haslinger · Donat Fäh · Domenico Giardini · Philipp Kästli · Urs Kradolfer · Iris Marschall · Stefan Wiemer

Received: 6 October 2010 / Accepted: 18 October 2010 / Published online: 30 November 2010
© Swiss Geological Society 2010

Abstract This report of the Swiss Seismological Service summarizes the seismic activity in Switzerland and surrounding regions during 2009. During this period, 450 earthquakes and 68 quarry blasts were detected and located in the region under consideration. The three strongest events occurred about 15 km NW of Basel in southern Germany (M_L 4.2), near Wildhaus in the Toggenburg (M_L 4.0) and near Bivio in Graubünden (M_L 3.5). Although felt by the population, they were not reported to have caused any damage. With a total of 24 events with $M_L \geq 2.5$, the seismic activity in the year 2009 was close to the average over the previous 34 years.

Keywords Earthquakes · Focal mechanisms · Moment tensors · Switzerland

Zusammenfassung Dieser Bericht des Schweizerischen Erdbebendienstes stellt eine Zusammenfassung der im Vorjahr in der Schweiz und Umgebung aufgetretenen Erdbeben dar. Im Jahr 2009 wurden im erwähnten Gebiet 450 Erdbeben sowie 68 Sprengungen erfasst und lokalisiert. Die drei stärksten Beben haben sich rund 15 km NW von Basel in Süddeutschland (M_L 4.2), bei Wildhaus im Toggenburg (M_L 4.0) und bei Bivio in Graubünden (M_L 3.5) ereignet. Mit nur 24 Beben der Magnitude $M_L \geq 2.5$, lag die seismische Aktivität im Jahr 2009 im Durchschnitt der vorhergehenden 34 Jahre.

Résumé Le présent rapport du Service Sismologique Suisse résume l'activité sismique en Suisse et dans les régions limitrophes au cours de l'année 2009. Durant cette période, 450 tremblements de terre et 68 tirs de carrière ont été détectés et localisés dans la région considérée. Les trois évenements les plus forts ont eu lieu environ à 15 km au NO de Bâle (M_L 4.2), près de Wildhaus dans le Toggenburg (M_L 4.0) et près de Bivio dans les Grisons (M_L 3.5). Avec 24 événements de magnitude $M_L \geq 2.5$, l'activité sismique de l'année 2009 est comparable à la moyenne des 34 années précédentes.

Introduction

Past earthquake activity in and around Switzerland has been documented in an uninterrupted series of annual reports from 1879 until 1963 (Jahresberichte des Schweizerischen Erdbebendienstes). Three additional annual reports have been published for the years 1972–1974. These reports together with historical records of earthquakes dating back to the 13th century have been summarized by Pavoni (1977) and provided the basis for the first seismic hazard map of Switzerland (Sägesser and Mayer-Rosa 1978). With the advent of routine data processing by computer, the wealth of data acquired by the nationwide seismograph network has been regularly documented in bulletins with detailed lists of all recorded

Editorial handling: S. Bucher.

N. Deichmann (✉) · J. Clinton · S. Husen · B. Edwards · F. Haslinger · D. Fäh · D. Giardini · P. Kästli · U. Kradolfer · I. Marschall · S. Wiemer
Swiss Seismological Service, ETH Zürich, Sonneggstrasse 5, 8092 Zurich, Switzerland
e-mail: deichmann@sed.ethz.ch
URL: http://www.seismo.ethz.ch

events (Monthly Bulletin of the Swiss Seismological Service). Since 1996, annual reports summarizing the seismic activity in Switzerland and surrounding regions have been published in the present form (Baer et al. 1997, 1999, 2001, 2003, 2005, 2007; Deichmann et al. 1998, 2000a, 2001, 2004, 2006, 2008, 2009). In the course of reassessing the seismic hazard in Switzerland, a new uniform earthquake catalog covering both the historical and instrumental periods has been compiled (Fäh et al. 2003). The data in this new Earthquake Catalog of Switzerland (ECOS) are available on line (http://www.seismo.ethz.ch, Swiss Earthquake Catalogs). The new seismic hazard map of Switzerland based on this catalog was officially released in 2004 (Giardini et al. 2004; Wiemer et al. 2009). In addition, numerous studies covering different aspects of the recent seismicity of Switzerland have been published in the scientific literature (for an overview and additional references see, e.g., Deichmann 1990; Pavoni and Roth 1990; Rüttener 1995; Rüttener et al. 1996; Pavoni et al. 1997; Deichmann et al. 2000b; Kastrup et al. 2004, 2007).

Data acquisition and analysis

Seismic stations in operation during 2009

The Swiss Seismological Service operates two separate nationwide seismic networks, a high-gain broad-band seismometer network (Fig. 1) and a low-gain accelerograph network. The former is designed to monitor continuously the ongoing earthquake activity down to magnitudes well below the human perception threshold, whereas the latter is principally aimed at engineering concerns and thus only records so-called strong motions. Beginning in 2003, efforts are underway to merge these two networks, primarily by upgrading the accelerograph network with strong-motion instruments capable of recording signals continuously and in real-time, together with the high-gain signals. First, 12 stations of the high-gain broad-band network have been equipped with an additional accelerometer ("BB, SM" in Table 1). Then as of 2006, 10 sites of the existing accelerometer network as well as several new sites have been equipped with modern sensors and digitizers featuring improved communication, higher dynamic range, broader frequency bandwidth and higher sensitivity ("SM" in Table 2). To monitor with greater precision an ongoing sequence of earthquakes in the immediate vicinity of the southern segment of the new Gotthard railway tunnel that is still under construction, a set of eight stations with short-period seismometers and in part with three-component accelerometers were installed during the late Fall of 2005 in the region between the Lukmanier Pass and the Leventina Valley (Table 2). Moreover, two accelerometers have been installed in the tunnel itself. At the beginning of 2008, an additional broad-band station (PIORA) was put into operation a few km north of this local network to monitor more closely potential seismicity associated with the northward

Table 1 High-gain seismograph stations of the Swiss national network (SDSNet) operational at the end of 2009

National on-line network recorded in Zurich		
Code	Station name	Type
ACB	Acheberg, AG	EB-3
AIGLE	Aigle, VD	BB-3
BALST	Balsthal, SO	BB-3
BERNI	Bernina, GR	BB-3
BNALP	Bannalpsee, NW	BB-3, SM-3
BOURR	Bourrignon, JU	BB-3, SM-3
BRANT	Les Verrières, NE	BB-3
DAVOX	Davos, GR	BB-3
DIX	Grande Dixence, VS	BB-3, SM-3
EMBD	Embd, VS	BB-3
EMV	Vieux Emosson, VS	BB-3, SM-3
FIESA	Fiescheralp	BB-3
FLACH	Flach, ZH	EB-3
FUORN	Ofenpass, GR	BB-3
FUSIO	Fusio, TI	BB-3, SM-3
GIMEL	Gimel, VD	BB-3
GRYON	Gryon, VS	EB-3
HASLI	Hasliberg, BE	BB-3
LIENZ	Kamor, SG	BB-3, SM-3
LKBD	Leukerbad, VS	EB-3
LKBD2	Leukerbad, VS	SP-3
LLS	Linth-Limmern, GL	BB-3, SM-3
MMK	Mattmark, VS	BB-3, SM-3
MUGIO	Muggio, TI	BB-3
MUO	Muotathal, SZ	BB-3
PLONS	Mels, SG	BB-3
SALAN	Lac de Salanfe, VS	EB-3
SENIN	Senin, VS	BB-3, SM-3
SLE	Schleitheim, SH	BB-3
STEIN	Stein am Rhein, SH	EB-3
SULZ	Cheisacher, AG	BB-3, SM-3
TORNY	Torny, FR	BB-3
TRULL	Trullikon, ZH	EB-3
VANNI	Vissoie, VS	BB-3
VDL	Valle di Lei, GR	BB-3, SM-3
WEIN	Weingarten, TG	EB-3
WILA	Wil, SG	BB-3
WIMIS	Wimmis, BE	BB-3
ZUR	Zürich-Degenried, ZH	BB-3, SM-3

Signals of LKBD2 are transmitted via analog telemetry

Instrument type: SP, 1-second; EB, 5-seconds; BB, broad band; SM, accelerometer; 3, vertical and horizontal components

Table 2 Strong-motion stations of the Swiss national network and local seismic networks with on-line data acquisition operational at the end of 2009

Code	Station name	Type
On-line strong-motion network		
OTTER	Otterbach, BS	SM-3
SAUR	Augst-Römermuseum, AG	SM-3
SBAF	Basel-Friedhofgasse, BS	SM-3
SBAP	Basel-PUK, BS	SM-3
SBAT	Basel-Tropenhaus, BS	SM-3
SBIS2	Binningen, BS	SM-3
SCEL	Celerina, GR	SM-3
SCOU	Cournillens, FR	SM-3
SCUC	Scuol-Clozza, GR	SM-3
SFRA	Frenkendorf, BL	SM-3
SIOO	Sion-Ophtalmologie, VS	SM-3
SIOV	Sion-Valere, VS	SM-3
SKAF	Kaiseraugst-Friedhof, AG	SM-3
SMUK	Muraz-Kläranlage, VS	SM-3
SMUR	Muraz-Reservoir, VS	SM-3
SMZW	Muttenz-Waldhaus, BL	SM-3
SRHB	Riehen–Bäumlihof, BS	SM-3
STAF	Tafers, FR	SM-3
STSP	Tschierv, GR	SM-3
SZER	Zernez, GR	SM-3
AlpTransit-Gotthard network		
CUNA	Cunera, GR	SP-3, SM-3
CURA	Curaglia, GR	SP-3
DOETR	Doetra, TI	SP-3, SM-3
LUKA1	Lucomagno, TI	SP-3, SM-3
MFSFA	Faido (Tunnel), TI	SM-3
PIORA	Piora (Tunnel), TI	BB-3
RITOM	Lago Ritom, TI	SP-3, SM-3
TONGO	Tortengo, TI	SP-3
Triemli geothermal network		
EWZT0	Triemli, ZH (228)	SP-3
EWZT1	Friedhof Wiedikon, ZH	SM-3
EWZT2	Wettswil, ZH	SP-3
EWZT3	Uitikon, ZH	SP-3
Basel borehole network		
HALTI	Haltingen (542)	SP-3
JOHAN	Sankt Johann (317)	SP-3
MATTE	Schützenmatte (553)	SP-3
OTER1	Otterbach (500)	BB-3, SM-3
OTER2	Otterbach (2740)	SP-3
Brigerbad geothermal station		
BIBA	Brigerbad, VS	SM-3

Instrument type: SP, 1 s; SM, accelerometer; 1, vertical component only; 3, vertical and horizontal components

The numbers in parentheses next to the borehole stations are the sensor depth with respect to ground surface in meters

progress of the tunnel construction. In 2009, two stations recording the data locally (CHAT1 and CHAT2) as well as one of the accelerometers installed in the tunnel itself (MSFB) were removed. In addition, two of the originally installed stations (NARA and CHIR2) were replaced by the two new stations CUNA and CURA, located closer to the tunnel segment under construction at that time. This eight-station network is operated under a contract with Alp-Transit-Gotthard AG.

In the course of 2006 an additional array of seismic sensors was installed in six boreholes at depths between 317 and 2,740 m below Basel (e.g., Deichmann and Ernst 2009). This array was designed to monitor the seismicity induced by the injection of large quantities of water at high pressure into a 5 km deep well in the context of a project initiated by Geopower Basel AG, a private/public consortium, to extract geothermal energy. In 2007, one of these six borehole stations (RIEH2) was removed and in 2009 the short-period sensor in OTER1 was replaced by a broadband instrument. Except for station OTER1, the borehole array is operated by Geothermal Explorers Ltd in Pratteln.

The earthquakes induced by the geothermal project in Basel has raised concerns about potential seismicity induced by other geothermal projects (even those that do not involve the enhancement of permeability through massive water injections). Therefore, it has become common practice to include local monitoring capabilities for such projects. As a consequence, in 2009 an additional accelerometer has been installed in Brigerbad, for a project to increase the geothermal productivity for a local spa, and an array of four stations was operated in and around the city of Zurich during an attempt by the local utility company (EWZ) to tap a possible aquifer at a depth of about 3 km (Table 2).

To improve the reliability of locations for events at the periphery or outside of Switzerland, we are engaged in an ongoing cross-frontier cooperative effort to exchange seismic data in real-time. Since 2005 we continuously record and archive signals from stations in Austria operated by the Zentralanstalt für Meteorologie und Geodynamik in Vienna (ZAMG) and in Italy operated by the Istituto Nazionale di Geofisica e Vulcanologìa in Rome (INGV), by the Istituto di Geofisica, Università di Genova, by the Zivilschutz der Autonomen Provinz Bozen-Südtirol (Baer et al. 2007) and by the Istituto Nazionale di Oceanografia e di Geofisica Sperimentale (OGS) in Trieste. The number of observed stations increases as new high-quality stations come on-line in the border region.

Hypocenter location, magnitude and focal mechanisms

Since the year 2005, hypocenter locations of most of the local earthquakes have been determined using the software

package NonLinLoc (Lomax et al 2000). The P-wave velocity model used was derived from a 3D tomographic inversion of local earthquake data with constraints from controlled source seismics (Husen et al. 2003), and the S-velocities are calculated from the P-velocity using a Vp/Vs ratio of 1.71.

Local magnitudes (M_L) are calculated from the maximum amplitude of the horizontal components of the digital broad-band seismograms filtered to simulate the response of a Wood-Anderson seismograph. The attenuation with epicentral distance is accounted for by an empirically determined relation (Kradolfer and Mayer-Rosa 1988). The final magnitude corresponds to the median value of all individual station magnitudes.

For the stronger events, the traditional determination of focal mechanisms from the azimuthal distribution of first-motion polarities (fault-plane solutions) is complemented by moment tensors based on full-waveform inversion. This procedure, based on a time domain inversion scheme developed by Dreger (2003), also provides a moment magnitude, M_w, the best fitting double couple, and an optimal depth estimate based on the given location.

Recently an additional procedure has been implemented that routinely and automatically provides estimates of M_w also for earthquakes of lower magnitudes. M_w values are computed using a spectral fitting technique following the method of Edwards et al. (2010). The far-field signal moments are obtained by simultaneously fitting the spectrum of a theoretical source model (Brune 1970, 1971) along with path-variable attenuation and event stress-drop to observed Fourier velocity spectra. The seismic moment is derived from the far-field signal moments assuming a simple geometrical spreading model that accounts for body and surface wave propagation. Site amplification is assumed negligible for the computation of M_w due to the predominant use of hard-rock recording sites.

A more detailed documentation of the data analysis can be found in previous annual reports (Deichmann et al. 2006, Baer et al. 2007).

Seismic activity during 2009

Overview

During 2009, the Swiss Seismological Service detected and located 450 earthquakes in the region shown in Fig. 2. Based on such criteria as the time of occurrence, the location, the signal character or on direct communication, 68 additional seismic events were identified as quarry blasts. The available faultplane solutions and moment tensors are shown in Fig. 3.

Magnitude values of the events recorded in 2009 range from M_L 0.2 to 4.2 (Fig. 4). The events with $M_L \geq 2.5$ and the criteria used to assign the quality rating for the given locations as well as the corresponding estimated location accuracy are listed in Tables 3 and 4. In addition to the parameters listed in previous annual reports, Table 3 includes also the available M_w values derived from the spectral fitting method of Edwards et al. (2010).

Figure 5 shows the epicenters of the 846 earthquakes with $M_L \geq 2.5$, which have been recorded in Switzerland and surrounding regions over the period of 1975–2009. These events represent about 8% of the total number of events detected during that time period in the same area. The chosen magnitude threshold of M_L 2.5 ensures that the

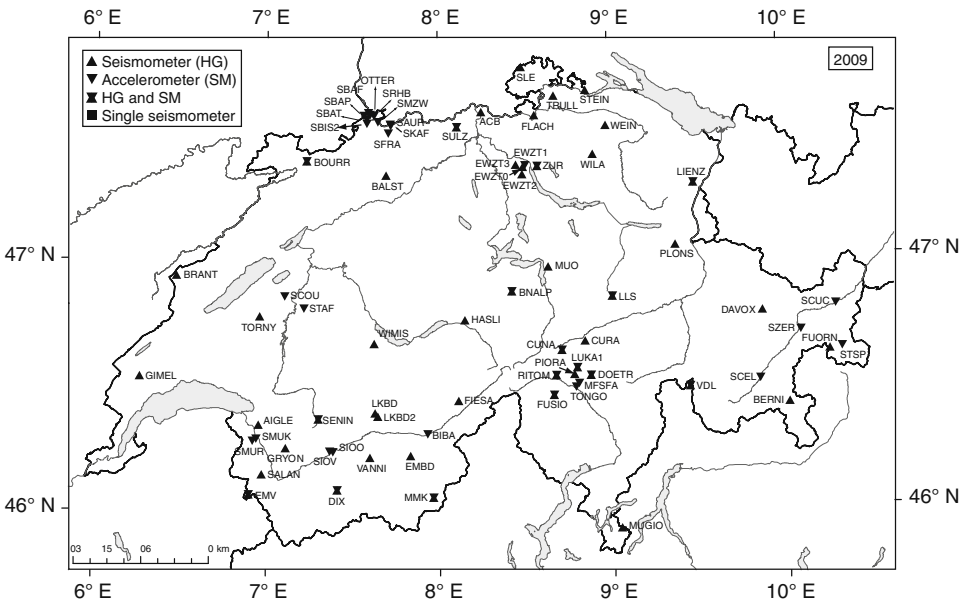

Fig. 1 Seismograph stations in Switzerland with on-line data acquisition operational at the end of 2009. The stations defined as high-gain (HG) are mostly equipped with broad-band or 5-s sensors, whereas the strong-motion stations (SM) are accelerometers. For a map of the Basel-borehole array see Baer et al. (2007) or Deichmann and Ernst (2009)

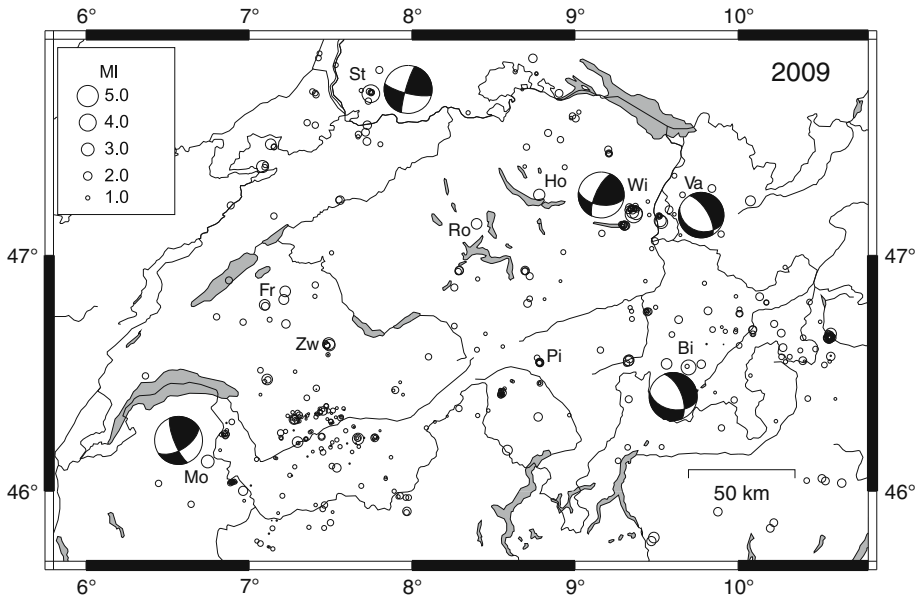

Fig. 2 Epicenters and focal mechanisms of earthquakes recorded by the Swiss Seismological Service during 2009. Epicenters of events mentioned in the text are Bivio (Bi), Fribourg (Fr), Hombrechtikon (Ho), Morzine (Mo), Root (Ro) Steinen (St), Vaduz (Va), Wildhaus (Wi) and Zwischenflüh (Zw)

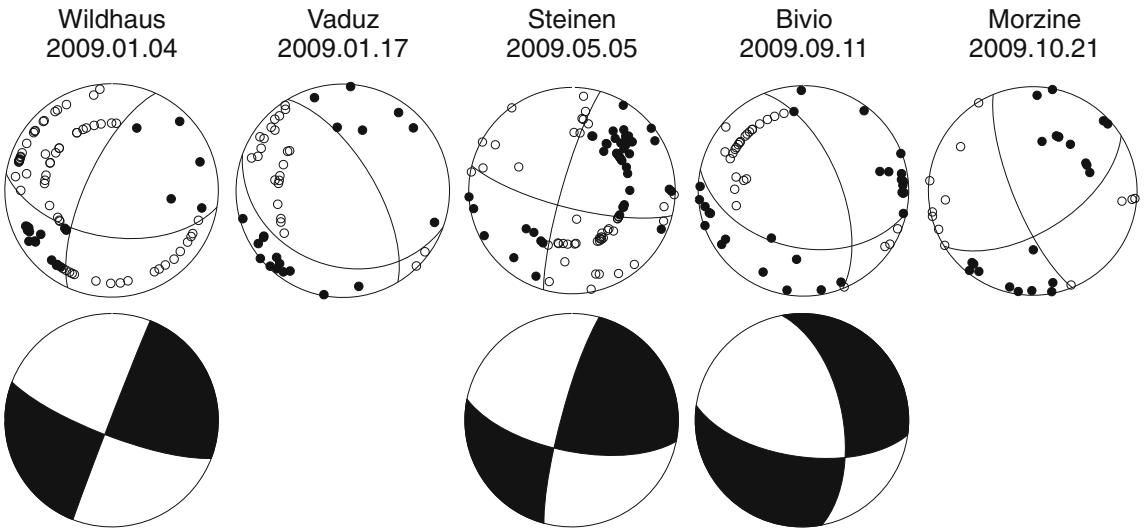

Fig. 3 Fault-plane solutions based on first-motion polarities (*above*) and optimal double-couple moment tensors based on full-waveform inversion (*below*). All stereographs are lower hemisphere, equal-area projections. *Solid circles* and *shaded quadrants* correspond to compressive first motion (*up*); *empty circles* and *white quadrants* correspond to dilatational first motion (*down*)

data set is complete for the given period and that the number of unidentified quarry blasts and of badly mislocated epicenters is negligible.

Significant earthquakes of 2009

Wildhaus

At 16:30 local time of January 4th, the Toggenburg was jolted by an earthquake with magnitude M_L 4.1. Its epicenter was located 3 km south of Wildhaus and it produced shaking of intensities IV (EMS) in the upper Toggenburg, Appenzell, the Rheintal of Sankt Gallen and Walensee area (Fig. 6). Maximum measured horizontal ground motions were recorded by an accelerometer near Gams (station SGAG), at an epicentral distance of 8 km, with values of 0.66 m/s^2 PGA and 19 mm/s PGV. A value for the moment magnitude of M_w 3.7 is obtained from the full-waveform moment tensor inversion and of M_w 4.0 from the spectral fitting method.

The hypocentral location based on the Swiss 3D velocity model of Husen et al. (2003) gives a focal depth of 4.5 km. This value is constrained by small travel-time residuals of both the Pn arrivals recorded at several distant stations and by the Pg and Sg arrivals at an accelerometer located on hard rock 6.3 km SW of the epicenter (station SBUM at Buchs-Malbun). The angle of incidence relative to vertical

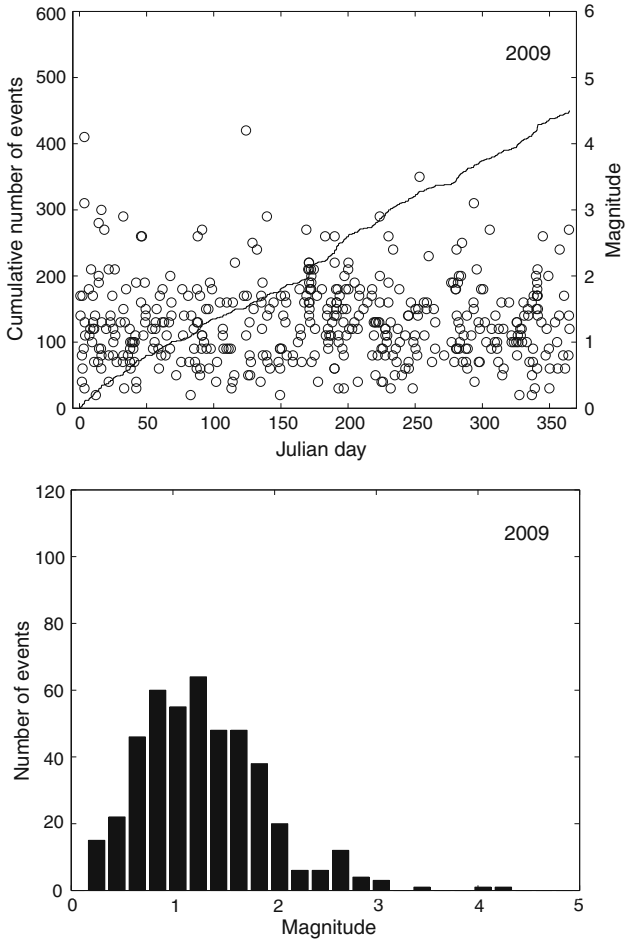

Fig. 4 Earthquake activity during 2009: magnitude of each event and cumulative number of events (*above*); histogram of magnitudes (*below*)

of the ray at this station, estimated from the polarization of the P-wave, is 52°. Assuming an average P-wave velocity Vp = 5 km/s and a ratio Vp/Vs = 1.8 for the sediments in the upper 5 km of the crust in this region, the observed S–P arrival-time difference of 1.3 s corresponds to a hypocentral distance of 8.1 km and to an epicentral distance of 6.3 km, in agreement with the result of the routine location procedure. The corresponding focal depth, assuming a straight ray path and taking into account the elevation of the station (1.4 km a.s.l), would correspond to a focal depth of 3.7 km. Even considering the uncertainties of the polarization measurement and of the assumed wave velocities, the two completely independent focal depth estimates are in very good agreement and lend confidence to the conclusion that the Wildhaus event occurred in the sedimentary cover, which in this region reaches a thickness of about 6 km (Hitz and Pfiffner 1997).

Given the relatively large magnitude of this event and the good station coverage, it was possible to construct a well-constrained fault-plane solution from the observed P-wave polarities. Take-off angles of the rays at the source were calculated with a 2D ray-tracing program along profiles of different azimuths, with a focal depth set to 4.5 km. The resulting focal mechanism is strike-slip with a small thrust component. The NNW-SSE oriented *P*-axis is consistent with the stress field derived from the analysis of earlier earthquakes in the Helvetic domain of eastern Switzerland (Kastrup et al. 2004). The horizontal orientation of the P- and T-axes of the moment tensor derived from the full-waveform inversion differs by a bit more than 10° from the fault-plane solution, and the moment tensor has a significantly smaller thrust component (Fig. 3; Table 5). Given that the waveform fit is excellent (variance reduction 85%) while the double couple component of the solution (70%) is relatively small, it is conceivable that the moment tensor inversion and the fault-plane solution look different because they are reflecting different aspects of the source.

Only 18 min later, the M_L 4.1 event was followed by an aftershock of M_L 3.1. This second event was the first of a total of 15 aftershocks recorded over the rest of the year 2009. One of these additional aftershocks, which occurred August 12th, reached a magnitude M_L 2.9; all others had magnitudes between 1.1 and 1.9. The routinely calculated hypocentral locations of the events comprising the entire sequence scatter over a relatively large volume. To a substantial extent this scatter is an artifact of the fact that the number and distribution of available stations is very different for the smaller and larger events. However, variations in the signal character among the individual events indicate that the true locations are likely to scatter as well. Preliminary results of a master-event relative location procedure, based on the manual arrival times read by the analyst, indicate that the epicenters could be distributed over an area of 2 × 3 km. The differences in signal character and clear polarity reversals at some key stations are evidence that the focal mechanisms of the mainshock and the two largest aftershocks are not identical either. However, the almost identical arrivaltime differences between the reflection at the Moho (PmP) and the direct wave (Pg) shown in Fig. 7, demonstrate that, at least for the three strongest events, the focal depths are practically the same. A more detailed analysis of the hypocentral distribution and focal mechanisms of the Wildhaus sequence is still underway.

Zwischenflüh

A sequence of six events occurred between January 15th and April 3rd near Zwischenflüh (BE), with magnitudes between M_L 1.0 and 2.8. The P-arrivals at most stations are rather emergent and also the S-arrivals are difficult to identify with confidence. The routine location procedure, based on the 3D velocity model, places the hypocenters of

Table 3 Earthquakes with $M_L \geq 2.5$

Date & Time UTC	Lat. (°N)	Lon. (°E)	X/Y (km)	Z (km)	Mag. ($M_{L)}$	Mag. (M_w)	Q	Location
2009.01.04 15:30:30	47.173	9.361	746/226	5	4.1	4.0	A	Wildhaus, SG
2009.01.04 15:48:47	47.176	9.375	747/227	5	3.1	3.1	A	Wildhaus, SG
2009.01.15 07:54:03	46.628	7.489	604/164	−2	2.8		B	Zwischenflüh, BE
2009.01.17 07:09:58	47.139	9.529	759/223	5	3.0	2.8	A	Vaduz, FL
2009.01.19 13:12:25	46.621	7.494	604/163	−2	2.7		B	Zwischenflüh, BE
2009.02.02 15:42:53	47.145	9.524	758/224	5	2.9	2.7	A	Vaduz, FL
2009.02.15 20:28:43	46.476	7.111	575/147	9	2.6	2.8	B	Château d'Oex, VD
2009.02.16 12:14:59	47.132	8.397	673/220	32	2.6	2.3	A	Root, LU
2009.03.30 01:39:54	47.464	7.134	577/257	22	2.6	2.6	A	Bonfol, JU
2009.04.02 08:54:15	47.234	6.471	527/232	7	2.7		C	Landresse, F
2009.05.05 01:39:25	47.674	7.748	623/280	12	4.2	3.7	A	Steinen, D
2009.05.09 20:54:58	46.210	7.299	589/118	7	2.5	2.5	A	Nendaz, VS
2009.05.20 13:19:09	47.372	7.083	573/247	5	2.9	2.8	B	Ocourt, JU
2009.06.18 23:03:02	46.669	10.570	840/173	10	2.7	2.6	A	Glorenza, I
2009.07.02 23:08:09	46.558	9.331	745/158	6	2.6	2.7	B	Splügen, GR
2009.07.10 01:06:47	45.802	9.485	759/074	13	2.6	2.6	B	Lecco, I
2009.08.12 13:52:28	47.181	9.354	745/227	4	2.9	3.0	A	Wildhaus, SG
2009.08.19 02:04:42	46.788	7.094	574/182	2	2.6	2.6	A	Matran, FR
2009.09.11 06:34:38	46.527	9.696	773/155	11	3.5	3.2	A	Bivio, GR
2009.10.12 21:56:03	46.542	9.562	763/157	7	2.5	2.3	A	Mulegns, GR
2009.10.21 16:10:59	46.128	6.747	547/109	6	3.1	3.0	A	Morzine, F
2009.11.02 12:14:35	47.253	8.780	701/234	32	2.7	2.4	A	Hombrechtikon, ZH
2009.12.12 00:17:48	46.844	7.222	584/189	2	2.6	2.7	A	Düdingen, FR
2009.12.31 10:49:36	46.224	7.669	618/119	6	2.7	2.8	B	Saint Luc, VS

The values listed under M_w are the moment magnitudes calculated from the spectral fitting method documented in Edwards et al. (2010). The focal depth of the events of Vaduz (2nd Feb.), Matran and Düdingen have been set manually to the given values as explained in the text. In some cases, where focal depths could be constrained by comparisons with neighboring events, quality B has been changed to quality A (see text for details)

Table 4 Criteria and location uncertainty corresponding to the quality rating (Q) of the hypocentral parameters in the event list

Rating	Criteria		Uncertainty	
Q	GAP (degrees)	DM (km)	H (km)	Z (km)
A	≤180	≤1.5 × Z	≤2	≤3
B	≤200	≤25	≤5	≤10
C	≤270	≤60	≤10	>10
D	>270	>60	>10	>10

GAP largest angle between epicenter and two adjacent stations; *DM* minimum epicentral distance; *H* horizontal location; *Z* focal depth

all six events at the Earth's surface. Although the location uncertainty is large, a shallow focal depth is in accord with the strong and long-lasting surface waves observed at several stations (in particular at station WIMIS at an epicentral distance of only about 12 km) and with the fact that the two events with M_L 2.7 and 2.8 were clearly felt by the local population. The first event was preceded by a small foreshock that occurred 3 s earlier. Two additional small events occurred in July and August about 4 km further to the south. The location algorithm puts them at a depth of 8 km. Although this value is also subject to a significant uncertainty, a larger focal depth is supported also by the higher frequency of the signals, the impulsive S-arrivals and large P-wave amplitudes on the vertical component at the closest station situated at an epicentral distance of 14 km. Thus, this doublet is not related to the earlier sequence.

Vaduz

The M_L 3.0 event, which occurred on January 17th at 8:10 in the morning local time right below the town of Vaduz, was part of a sequence of eight events that began 7 h earlier with a M_L 0.9 event. It was followed that same day by two more small events (M_L 0.8 and 1.3). For the mainshock there are

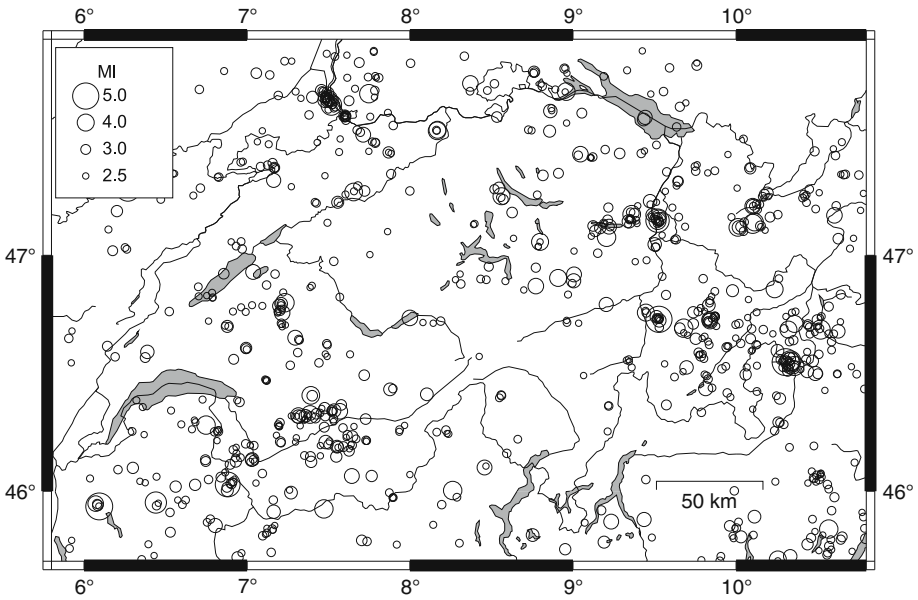

Fig. 5 Epicenters of earthquakes with Magnitudes $M_L \geq 2.5$, during the period 1975–2009

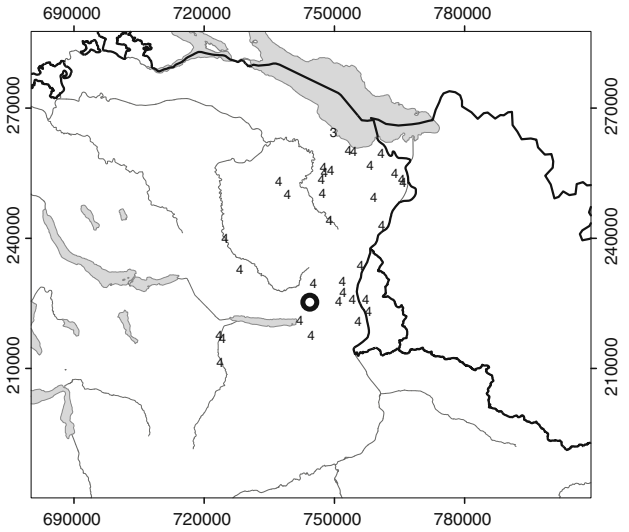

Fig. 6 Macroseismic intensities (EMS98) for the M_L 4.1 event near Wildhaus (SG). The Swiss cartesian coordinates are labeled in m

37 reports of it having been felt. After 2 weeks of quiescence, activity picked up again in the afternoon of February 2nd with two events with magnitudes M_L 2.9 and 1.5. Two additional small events (M_L 1.0 and 0.9) occurred February 10th and 24th. All eight events have very similar waveforms, typical of nearly colocated events with identical focal mechanisms. The scatter in the routinely determined locations (3 km horizontally and 10 km in depth) is clearly an artifact of the different station distribution available for the location of the stronger and weaker events, and thus of the poorly constrained locations of the latter. The 4.7 km focal depth of the mainshock is based on the Swiss 3D model and relies on P- and S-arrivals recorded by an accelerometer at an epicentral distance of 5 km as well as on several Pn arrivals observed at distances between 140 and 216 km. The similarity of the focal depth of the Vaduz and Wildhaus events is confirmed by 2D ray-trace modelling of the PmP-Pg travel-time differences observed at stations TRULL and SLE (at epicentral distances between 73 and 105 km).

The fault-plane solution, based on first-motion polarities, corresponds to a normal faulting mechanism with a NE-SW oriented T-axis. This mechanism is constrained to a large degree by the upward motion of the arrival at station ABSI, located in northern Italy, at a distance of 144 km ESE of the epicenter. Without this observation, the focal mechanism could also be strike-slip. For this reason, we not only checked that the seismometer was operating correctly, but, to verify that the identified first motion really corresponds to the first arrival, we also compared the observed travel time at station ABSI with the travel times at neighboring stations for the Vaduz mainshock and with the travel times observed for the M_L 4.1 Wildhaus event. As a result, we have no reason to question the reliability of the first-motion polarity observed at station ABSI, and conclude that the focal mechanism derived for the Vaduz sequence is well constrained. It is noteworthy, because it constitutes the first normal-fault mechanism observed in this region. Whereas the hypocenters of the Wildhaus earthquakes are certainly located in the Helvetic Nappes, those of the Vaduz sequence might be located in a transition zone between the Helvetic and the Austro-Alpine Nappes (Hitz and Pfiffner 1997).

Steinen

The epicenter of the earthquake that occurred at 03:39 (local time) of May 5th was located about 15 km NW of

Table 5 Focal mechanism parameters based on first-motion polarities (lines with M_L) and on an automated full-waveform inversion method (lines with M_w)

Location	Date & Time (UTC)	Depth (km)	Mag.	Strike/dip/rake		Az/dip	
				Plane 1	Plane 2	*P*-axis	*T*-axis
Wildhaus	2009/01/04 15:31	4	M_L 4.1	099/54/155	204/70/039	328/10	067/41
		5	M_w 3.7	111/78/179	201/89/012	335/08	067/09
Vaduz	2009/01/17 07:10	5	M_L 3.0	110/30/−125	329/66/−072	270/64	045/19
Steinen	2009/05/05 01:39	12	M_L 4.2	104/76/172	196/82/014	329/04	061/16
		8	M_w 3.6	101/66/171	195/82/024	326/11	061/23
Bivio	2009/09/11 06:35	11	M_L 3.5	102/45/−137	338/61/−054	299/57	043/09
		8	M_w 3.1	094/55/−148	345/64/−039	306/45	042/05
Morzine	2009/10/21 16:11	6	M_L 3.7	058/58/162	158/75/033	285/11	022/34

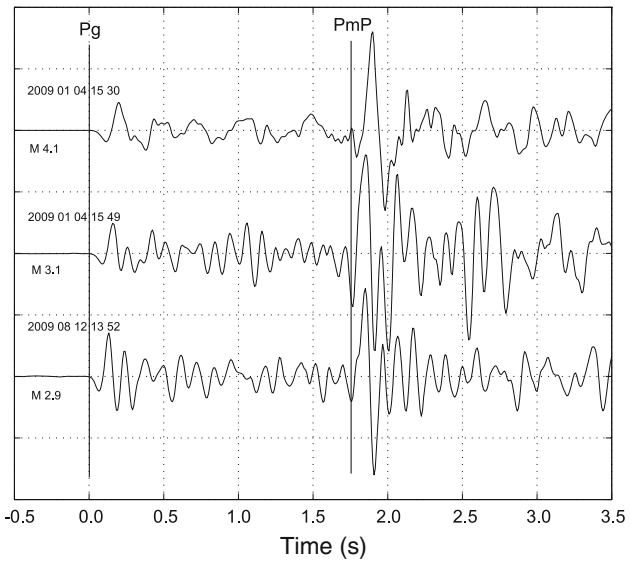

Fig. 7 Seismograms of the three strongest Wildhaus events recorded at station SLE (Bandpass filter 2–20 Hz) The almost identical arrival-time difference between the reflection from the Moho (PmP) and the direct wave (Pg) implies that the focal depth of the three events is also practically the same

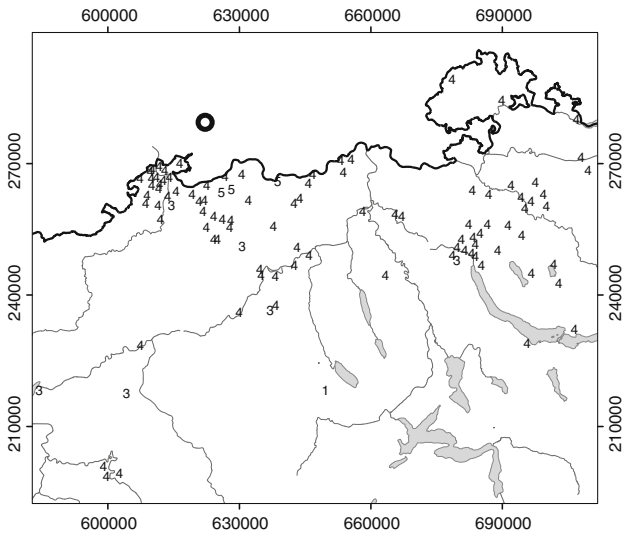

Fig. 8 Macroseismic intensities (EMS98) for the M_L 4.2 event near Steinen (D). The Swiss cartesian coordinates are labeled in m

Basel, near the village of Steinen in southern Germany. With a focal depth of 12 km and a magnitude M_L 4.2 it produced maximum intensities in Switzerland of V (EMS) and, despite its occurrence in the middle of the night, was clearly felt with intensities of IV across most of northern Switzerland (Fig. 8) as well as over large parts of south-western Germany and the bordering regions of France. The maximum values of measured horizontal ground motion were recorded by an accelerometer near Frenkendorf (SFRA) located at an epicentral distance of 19 km, with values of 0.54 m/s^2 (PGA) and 14 mm/s (PGV). At the site closest to the epicenter, for which records are available (station END, distance of 5 km), maximum horizontal ground motion reached 0.41 m/s^2 (PGA) and 5.6 mm/s (PGV).

With 19 stations within an epicentral distance range of 5–20 km and with numerous impulsive arrivals visible out to distances beyond 250 km, the hypocentral location of this event based on the Swiss 3D velocity model is very reliable. Though there are some discrepant polarities near the nodal planes, the fault-plane solution is similarly well constrained and agrees closely with the results of the full-waveform inversion for the moment tensor (Fig. 3; Table 5). The latter features a double-couple component of 91% and a variance reduction of 83%, with a moment magnitude M_w of 3.6. Both solutions correspond to a strike-slip mechanism with NNW-SSE and ENE-WSW oriented P- and T-axes, in accord with the orientation of the known regional stress field (e.g., Kastrup et al. 2004).

In the 5 days following this event, the Swiss Seismological Service recorded three aftershocks (M_L between 1.1 and 1.5), and a fourth aftershock (M_L 1.1) was recorded in September. An additional three events, with M_L between

1.0 and 1.6, occurred nearby in April, July and October, but at significantly larger focal depths, so that they can not be regarded as aftershocks of the May 5th event.

Bivio

The M_L 3.5 event that occurred on Sept. 11th near Bivio triggered the off-line accelerometers located in Bergün (SBET) and in Celerina (SCEM) at epicentral distances of 9 and 11 km. Peak horizontal ground motion recorded by these two instruments, which are located on hard rock, reached 0.23 m/s^2 and 0.06 m/s^2 (PGA) and 4.6 mm/s and 2.0 mm/s (PGV). There are 47 reports of it having been felt, mostly from the Engadine and central Graubünden.

Given a favorable azimuthal station coverage, the epicentral location is well constrained and insensitive to using different velocity models and different distance cut-offs for the stations used by the location algorithm. Focal depth, on the other hand, varies between 6 and 11 km, depending on whether one uses arrivals out to distances of more than 250 km or uses a distance cut-off of 72 km. The shallower focal depth is constrained by the Pn arrivals observed at larger distances and results in unusually large travel-time residuals of both P and S-arrivals at the closest stations. Without the Pn arrivals, the calculated focal depth increases to 11 km and the residuals at the closer stations decrease to normal values. A focal depth beyond 10 km agrees also with the qualitative observation that the travel-time curve plotted through the arrival times as a function of epicentral distance is strongly curved out to distances of about 30 km. If the depth were around 6 km, the pronounced curvature of the travel-time curve would not be observed beyond about 15 km. In addition, 2D ray-tracing, using as reference the well-constrained 8 km focal depth of the M_L 4.0 Paspels event of 2008, located 31 km NW of Bivio, results in a focal depth for the Bivio event between 9 and 12 km.

Thus, the take-off angles of the rays at the source used by the fault-plane solution, were calculated for a focal depth of 11 km. The result is a normal faulting mechanism with a NE–SW oriented T-axis and agrees with the moment tensor obtained from the low-frequency full-waveform inversion to within <10° (Fig. 3; Table 5). The moment magnitude associated with the latter is M_w 3.1. Both the type of mechanism and the orientation of the T-axis is typical for the Penninic domain of Graubünden (Roth et al. 1992, Kastrup et al. 2007).

The Bivio event was preceded on February 17th by a foreshock with M_L 1.1; two additional aftershocks occurred in 2010, with magnitudes M_L 2.0 and 1.1.

Morzine

The M_L 3.1 event that occurred October 21st, close to the town of Morzine, just across the border with France, is interesting because its epicenter is located near the events of Samoëns (2000.08.19, M_L 3.3) and Vallorcine (2005.09.08, M_L 4.9), for which detailed studies are available (Delacou et al. 2005; Fréchet et al. 2010). The epicentral location based on data from both the Swiss national network and the SISMALP stations, operated by the University of Grenoble, is reliable, and the focal depth of 6 km is well-constrained by observations at station OG03, located at an epicentral distance of only 7 km, as well as by a good azimuthal station distribution. Take-off angles for the fault-plane solutions were set equal to those of the Samoëns event, which had a similar focal depth (5 km) and for which the take-off angles were derived from 2D ray-tracing (Delacou et al. 2005). The result is a strike-slip mechanism with P- and T-axes oriented WNW-ESE and NNE-SSW, that is very similar to the mechanism of the Vallorcine event of 2005 (Fréchet et al. 2010). The mechanism of the Samoëns event is also strike-slip, but the P- and T-axes are oriented NW–SE and NE–SW.

Fribourg

The year 2009 saw four events with magnitudes M_L 1.9–2.6 occurring within a radius of about 6 km from the city of Fribourg. Although their magnitudes are small, they are interesting because in the years 1987, 1995, and 1999 the area of Fribourg has seen repeated sequences of earthquakes, that have reached magnitudes M_L up to 4.3 and that seem to delineate an active, several km long N–S trending fault zone east of the city (Kastrup et al. 2007). As a consequence, in 2008, the Canton of Fribourg commissioned the Swiss Seismological Service to install two additional accelerometers near Cournillens (SCOU) and near Tafers (STAF), which, as shown by the example in Fig. 9, have provided excellent records of these new events.

Two of the four events recorded in 2009 occurred within 32 min from each other in the early morning hours of August 19th near the town of Matran, west of the city of Fribourg. Therefore, these two events are not in any way related to the earlier earthquake sequences east of Fribourg. The M_L 2.4 event of May 13th near Tafers and the M_L 2.6 event of December 12th near Düdingen, on the other hand, occurred along the northward continuation of the lineament defined by the epicenters of the earthquake sequences of 1987, 1995, and 1999. In fact, both the routinely performed absolute locations and the results of a master-event location procedure place the epicenters of the Tafers and Düdingen events 2–2.5 and 5.5–6 km north of the M_L 4.3 event of 1999.

The routinely determined locations were calculated with program NonLinLoc and the Swiss 3D model (Husen et al. 2003), using the EDT option, that down-weights arrivals

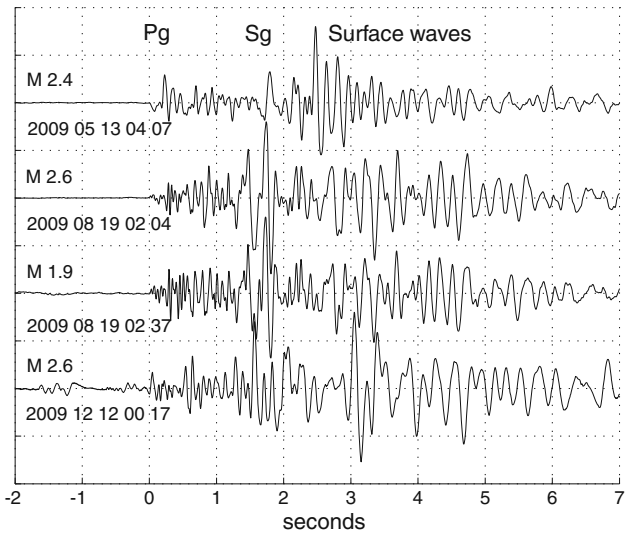

Fig. 9 Seismograms of the four Fribourg events recorded at station SCOU, integrated to velocity and filtered with a 2nd order band-pass filter between 1 and 20 Hz. From top to bottom, the signals correspond to the events of Tafers, Matran (2) and Düdingen. Epicentral distances vary between 7.5 and 10 km. The pronounced surface waves observed at such short epicentral distances are typical of events with hypocenters at depths of only a few km within the sedimentary layers

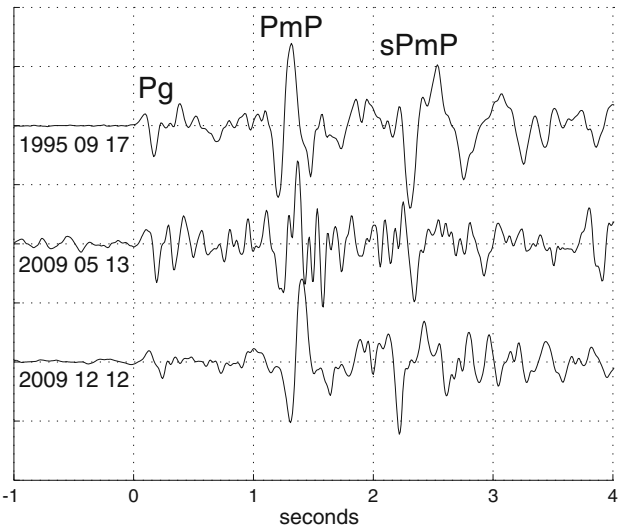

Fig. 10 Seismograms of one of the 1995 Fribourg events (*top*) and the 2009 events of Tafers (*middle*) and Düdingen (*bottom*) recorded at station ACB (epicentral distance between 114 and 119 km). The almost identical arrival-time differences between the sPmP and the PmP phases shows that the focal depth of all three events must be similar

with large residuals. In the case of the four events considered here, the down-weighting applies to the S-arrivals recorded at distances between about 10 and 80 km and to the P-arrivals recorded at distances beyond about 100 km. For the Tafers and Düdingen events, the resulting focal depths are 3.5 and 4.1 km. Based on synthetic seismograms, Kastrup et al. (2007) showed that the travel-time differences between the direct reflection at the Moho (PmP) and the reflection at the Moho originating from the conversion of the S-wave at the Earth's surface (sPmP), observed for the events recorded in 1995 and 1999, could be explained best for a focal depth of about 2 km. In Fig. 10 we show that the PmP and the sPmP phases of the 1995 Fribourg event and the two events of Tafers and Düdingen recorded in 2009 at station ACB are very similar, and that therefore the focal depths of the 2010 events are likely to be close to 2 km as well. A shallow focal depth is also compatible with the S–P travel-time difference of only 0.7 s observed for the Tafers event at station STAF, located at an epicentral distance of about 1 km, as well as with the fact that the Düdingen event was felt by several people, despite its small magnitude (M_L 2.6) and its occurrence in the mddle of the night.

In the case of the Matran events, the routinely calculated focal depths are nearly 6 km for the M_L 2.6 event and at the Earth's surface for the M_L 1.9 event. However, given the high similarity of the waveforms of the two Matran events (see e.g., traces 2 and 3 in Fig. 9) the two hypocenters must be nearly identical, and the obtained focal depth differences must be an artifact of the location procedure. In fact, the larger focal depth of the M_L 2.6 event is mainly constrained by the phase refracted at the Moho (Pn) observed at several stations in north-eastern Switzerland at distances beyond about 120 km. For the weaker M_L 1.9 event these Pn arrivals are below the noise level, so that its focal depth is mathematically poorly constrained. In fact neither value is correct. A comparison of the arrival time differences between the PmP and the Pg phases observed for the stronger of the two Matran events and for the Düdingen event at almost the same epicentral distance (Fig. 11) shows that the most likely focal depth of the Matran events must also be around 2 km. As in the case of the Düdingen event, the first Matran event, despite its low magnitude and its occurrence in the early morning hours, was felt by several people, which again suggests that its source was shallow.

Due to the small magnitudes and the shallow focal depth of these four events, the onset of the P-phase is often emergent and does not rise clearly above the noise at larger distances. Therefore, reliable first-motion polarities are too few to derive well-constrained focal mechanisms. Nevertheless, the available observations are not incompatible with a strike slip mechanism, with more or less N–S and E-W oriented fault planes (Fig. 12). Such a mechanism would be similar to the focal mechanisms of the 1987, 1995, and 1999 earthquake sequences (Kastrup et al. 2007) and compatible with the regional stress field (Kastrup et al. 2004).

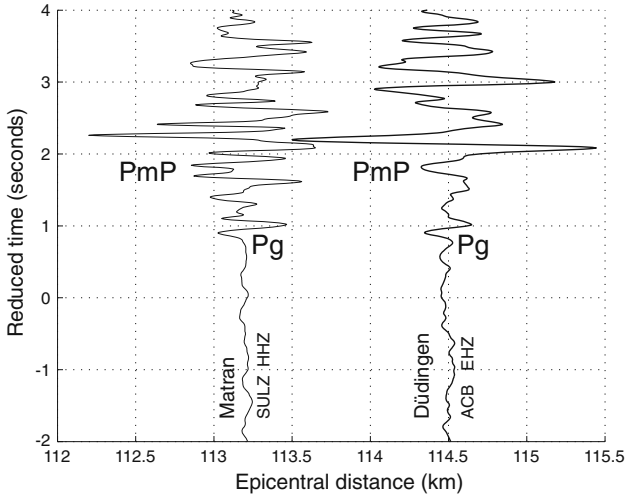

Fig. 11 Seismograms of the M_L 2.6 Matran event recorded at station SULZ and of the M_L 2.6 Düdingen event recorded at station ACB. Given the nearly identical epicentral distances of the two stations and a nearly horizontal Moho along the segement where the PmP reflection occurs (Waldhauser et al. 1998), the almost identical arrival-time differences between the PmP and the Pg phases shows that the focal depth of the two events must be similar

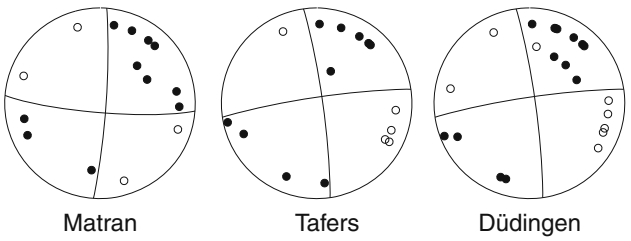

Fig. 12 Faultplane solutions (lower hemisphere, equal area projection) for the Tafers, Matran and Düdingen events of 2009. Take-off angles of the rays at the source are consistent with those calculated by Kastrup et al. (2007) for the Fribourg sequences of 1987, 1995 and 1999. The discrepant observation (*Down*) for the Düdingen event is station STAF, at an epicentral distance of only 4 km, and could therefore be due to a slight error in location and consequently in the calculated azimuth of the ray

In conclusion, the four events of 2009 near the city of Fribourg demonstrate that the seismic activity observed in the past within the near-surface sedimentary layers in this area is ongoing. Moreover, the results of the analysis of the Tafers and Düdingen events constitute evidence for a northward extension of the N–S striking fault zone, as defined by the earthquake sequences of 1987, 1995, and 1999 and postulated by Kastrup et al. (2007).

Piora

During 2009 the AlpTransit network recorded 51 earthquakes with local magnitudes between 0.2 and 2.0 in the Piora region. Of these 51 earthquakes, six earthquakes were strong enough to be detected by the SDSNet. Activity was spread over the entire year with a strong peak in December 2009, when 14 earthquakes occurred within 3 days. All earthquakes occurred north of the Piora zone in the vicinity of the Gotthard base-tunnel, which was under construction at that time. Recorded waveforms show a strong similarity within different groups of events, suggesting that several fault patches ruptured repeatedly. Overall, seismicity migrated from south to north during the year, in accordance with the progression of construction work. Although some earthquakes were accompanied by rock bursts in the tunnel, no obvious correlation was observed between rock bursts and earthquake activity. Given the close temporal and spatial correlation, however, it is likely that the earthquake activity has been induced by the construction work of the Gotthard base-tunnel.

Landslides

On April 19th, at 11:05, 23:35, and 23:43 (local time), the Swiss high-gain seismic network was triggered by three events with emergent and long-lasting signals, typical of large landslides (Fig. 13). Because of the emergent character of the signal onsets, in particular of the first two events, their source location was difficult to determine with confidence. However, the signals of the third event contain one or two more impulsive phases, that can be identified in seismograms recorded at several stations (see e.g., Fig. 13). Interpreting these phases as P- and S-waves gives a reasonably consistent epicenter location in the region of Pizzo Fiorera, on the border between Val Bavona (Ticino) and Val Formazza (Italy). The equivalent magnitudes of these events are M_L 2.2, 1.7, and 2.1. Interestingly, despite its low M_L value, the first event triggered the automatic moment tensor inversion algorithm, resulting in an unusual focal mechanism, with a double-couple component that corresponds to a thrust event with more or less horizontal and vertical nodal planes. The reason that this small event triggered the full-waveform inversion is that, as is shown in Fig. 13, its signals are unusually large at the low frequencies normally used for such an inversion. The corresponding equivalent moment magnitude M_w is 3.5. Such a high M_w value is not consistent with an M_L 2.2 earthquake and is further evidence for the fact that this and the other three events must be landslides. Only much later was it confirmed that these signals were caused by a massive landslide that descended that day in at least three phases from the western flanks of Pizzo Fiorera, at an altitude of about 1800 m a.s.l., and almost reached the first houses of Ponte in Val Formazza, located about 500 m lower on the floor of the valley.

Discussion

In 2009, as in previous years, in terms of the number of events most of the earthquakes occurred in the Valais and

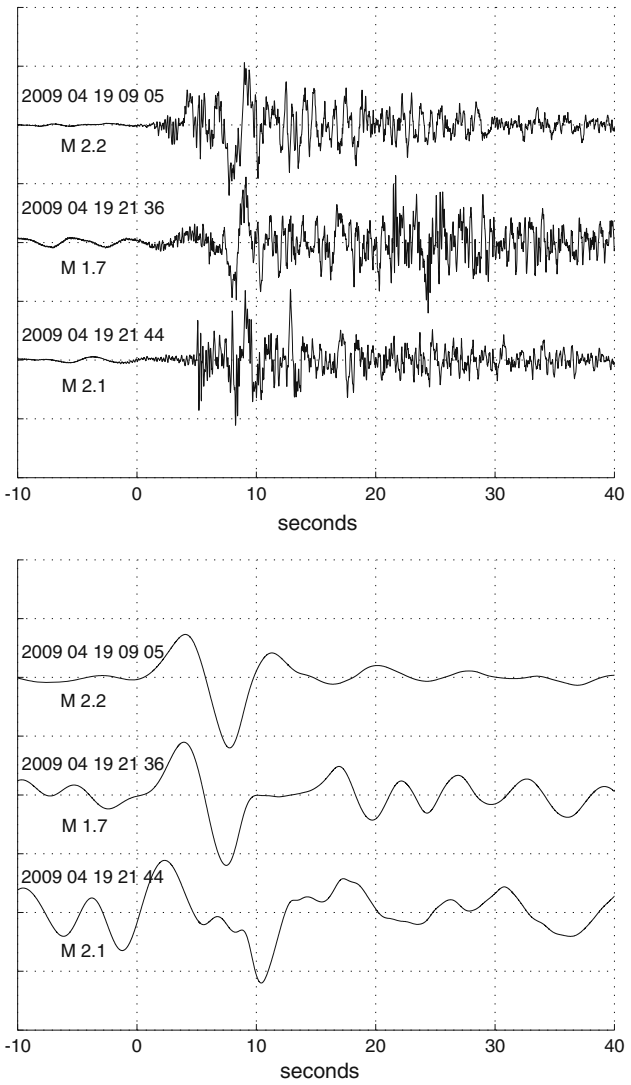

Fig. 13 Seismograms (vertical component, ground velocity) of the three landslides in Val Formazza recorded at station FUSIO (distance 20 km), approximately aligned at the onset of the signals (*top*: unfiltered; *bottom*: 4th order, zero-phase, band-pass filter 0.025–0.1 Hz). Note the more impulsive arrivals in the third unfiltered trace, visible at 5 and 8 s after the onset. In the filtered traces, the signal of the third event barely rises above the background noise, but in the seismograms of the first and second event it is clearly visible

in Graubünden. However, the two strongest events with $M_L \geq 4$ occurred northeast of Basel and in the Toggenburg. Routinely calculated focal depths for all but 17 events recorded in 2009 are <16 km. Of the deeper hypocenters, 15 are below the Molasse Basin and Jura of northern Switzerland and southern Germany; one with a depth of 24 km occurred in the Voralberg region (Austria) and one near Camedo, on the border between the Canton Ticino and Italy. The focal depth (23 km) of the latter is poorly constrained, given the sparse station coverage in that region and the complex crustal structure in the vicinity of the Ivrea Body. The two deepest events (near Root, LU, and Hombrechtikon, ZH, Switzerland) were located at depths of 32 km, which puts them just above the Moho, situated at about 34 km in these two locations (Waldhauser et al. 1998). The proximity to the Moho of these two hypocenters is well constrained by the fact that the Pn phase appears as the first arrival already at epicentral distances <50 km. Of the 450 earthquakes recorded in 2009, 16 were part of the Wildhaus cluster and 9 were part of the Vaduz sequence. The seismic activity induced by the geothermal project in Basel in 2006 and 2007 (e.g., Deichmann and Ernst 2009; Deichmann and Giardini 2009) continued to decrease over the year 2009, and the events that have been recorded by the local borehole seismometers were too weak to be detected by the national broad-band network. The total number of 24 events with $M_L \geq 2.5$ was about equal to the yearly average over the previous 34 years in this magnitude category.

Acknowledgments Monitoring the seismicity in a small country is not possible without international cooperation. We thank W. Brüstle and S. Stange of the Erdbebendienst des Landesamtes für Geologie, Rohstoffe und Bergbau Baden-Württemberg in Freiburg, who kindly responded to our requests for information and data in 2009. Thanks also to R. Widmer and the Bundesanstalt für Geologie und Rohstoffe, Germany, for enabling access to the data of station BFO. Automatic data exchange in real-time has been implemented with the Zentralanstalt für Meteorologie und Geodynamik in Vienna, with the Istituto Nazionale di Geofisica e Vulcanologìa in Rome and with the Zivilschutz der Autonomen Provinz Bozen-Südtirol. Access to the data of the borehole sensors in Basel was granted by Geopower Basel AG, and we thank Geothermal Explorers Ltd for their help. We are also very grateful to P. Zweifel and our colleagues in the SED electronics lab for their relentless efforts in ensuring the continuous reliability of the data acquisition systems, and to S. Räss and A. Blanchard for administrative and logistic support. Financial support from the Nationale Genossenschaft für die Lagerung radioaktiver Abfälle, Nagra, for the operation of the stations in northeastern Switzerland, as well as from AlpTransit-Gotthard AG for the operation of the network around the southern segment of the new Gotthard Tunnel is gratefully acknowledged. Station BIBA was installed under contract with Thermalbad-Brigerbad, and the Triemli geothermal network was financed by the Elektrizitätswerke der Stadt Zürich (EWZ). We thank the Etablissement cantonal d'assurance des bâtiments (ECAB) of the Canton of Fribourg for having financed stations SCOU and STAF, which contributed very valuable data for the analysis of the four Friburg events in 2009. We are grateful to Franziska Dammeier and Jeff Moore for finding the confirmation of the Val Formazza landslide.

References

Baer, M., Deichmann, N., Ballarin Dolfin, D., Bay, F., Delouis, B., Fäh, D., et al. (1999). Earthquakes in Switzerland and surrounding regions during 1998. *Eclogae Geologicae Helvetiae, 92*(2), 265–273.

Baer, M., Deichmann, N., Braunmiller, J., Ballarin Dolfin, D., Bay, F., Bernardi, F., et al. (2001). Earthquakes in Switzerland and surrounding regions during 2000. *Eclogae Geologicae Helvetiae, 94*(2), 253–264.

Baer, M., Deichmann, N., Braunmiller, J., Bernardi, F., Cornou, C., Fäh, D., et al. (2003). Earthquakes in Switzerland and surrounding regions during 2002. *Eclogae Geologicae Helvetiae—Swiss Journal of Geosciences, 96*(2), 313–324.

Baer, M., Deichmann, N., Braunmiller, J., Clinton, J., Husen, S., Fäh, D., et al. (2007). Earthquakes in Switzerland and surrounding regions during 2006. *Swiss Journal of Geosciences, 100*(3), 517–528. doi:10.1007/s00015-007-1242-0.

Baer, M., Deichmann, N., Braunmiller, J., Husen, S., Fäh, D., Giardini, D., Kästli, P., Kradolfer, U., Wiemer, S. (2005). Earthquakes in Switzerland and surrounding regions during 2004. *Eclogae Geologicae Helvetiae–Swiss Journal of Geosciences*, *98*(3), 407–418. doi:10.1007/s00015-005-1168-3.

Baer, M., Deichmann, N., Fäh, D., Kradolfer, U., Mayer-Rosa, D., Rüttener, E., et al. (1997). Earthquakes in Switzerland and surrounding regions during 1996. *Eclogae Geologicae Helvetiae, 90*(3), 557–567.

Brune, J. N. (1970). Tectonic stress and the spectra of seismic shear waves from earthquakes. *Journal of Geophysical Research, 75*, 4997–5010.

Brune, J. N. (1971). Correction: tectonic stress and the spectra of seismic shear waves from earthquakes. *Journal of Geophysical Research, 76*, 5002.

Deichmann, N. (1990). Seismizität der Nordschweiz, 1987–1989, und Auswertung der Erdbebenserien von Günsberg, Läufelfingen und Zeglingen. *Nagra Technischer Bericht*, NTB 90-46, Baden: Nagra.

Deichmann, N., Baer, M., Ballarin Dolfin, D., Fäh, D., Flück, P., Kastrup, U., et al. (1998). Earthquakes in Switzerland and surrounding regions during 1997. *Eclogae Geologicae Helvetiae, 91*(2), 237–246.

Deichmann, N., Baer, M., Braunmiller, J., Ballarin Dolfin, D., Bay, F., Bernardi, F., et al. (2002). Earthquakes in Switzerland and surrounding regions during 2001. *Eclogae Geologicae Helvetiae—Swiss Journal of Geosciences, 95*(2), 249–261.

Deichmann, N., Baer, M., Braunmiller, J., Ballarin Dolfin, D., Bay, F., Delouis, B., et al. (2000a). Earthquakes in Switzerland and surrounding regions during 1999. *Eclogae Geologicae Helvetiae, 93*(3), 395–406.

Deichmann, N., Baer, M., Braunmiller, J., Cornou, C., Fäh, D., Giardini, D., et al. (2004). Earthquakes in Switzerland and surrounding regions during 2003. *Eclogae Geologicae Helvetiae—Swiss Journal of Geosciences, 97*(3), 447–458.

Deichmann, N., Baer, M., Braunmiller, J., Husen, S., Fäh, D., Giardini, D., et al. (2006). Earthquakes in Switzerland and surrounding regions during 2005. *Eclogae Geologicae Helvetiae—Swiss Journal of Geosciences, 99*(3), 443–452. doi:10.1007/s00015-006-1201-1.

Deichmann, N., Baer, M., Clinton, J., Husen, S., Fäh, D., Giardini, D., et al. (2008). Earthquakes in Switzerland and surrounding regions during 2007. *Swiss Journal of Geosciences, 101*(3), 659–667. doi:10.1007/s00015-008-1304-y.

Deichmann, N., Ballarin Dolfin, D., & Kastrup, U. (2000b). Seismizität der Nord- und Zentralschweiz. *Nagra Technischer Bericht*, NTB 00-05, Nagra, Wettingen.

Deichmann, N., Clinton, J., Husen, S., Haslinger, F., Fäh, D., Giardini, D., et al. (2009). Earthquakes in Switzerland and surrounding regions during 2008. *Swiss Journal Geosciences, 102*(3), 505–514. doi:10.1007/s00015-009-1339-8.

Deichmann, N., & Ernst, J. (2009). Earthquake focal mechanisms of the induced seismicity in 2006 and 2007 below Basel (Switzerland). *Swiss Journal of Geosciences, 102*(3), 457–466. doi:10.1007/s00015-009-1336-y.

Deichmann, N., & Giardini, D. (2009). Earthquakes induced by the stimulation of an enhanced geothermal system below Basel (Switzerland). *Seismological Research Letters, 80*(3), 784–798. doi:10.1785/gssrl.80.5.784.

Delacou, B., Deichmann, N., Sue, C., Thouvenot, F., Champagnac, D., & Burkhard, M. (2005). Active strike-slip faulting in the Chablais area (NW Alps) from earthquake focal mechanisms and relative locations. *Eclogae Geologicae Helvetiae—Swiss Journal Geosciences, 98*(2), 189–199. doi:10.1007/s00015-005-1159-4.

Dreger, D. S. (2003). TDMT INV: time domain seismic moment tensor INVersion. In: W. H. K. Lee, H. Kanamori, P. C. Jennings, & C. Kisslinger (Eds.), *International handbook of earthquake and engineering seismology*, *B*, 1627.

Edwards, B., Allmann, B., Fäh, D., & Clinton, J. (2010). Automatic computation of moment magnitudes for small earthquakes and the scaling of local to moment magnitude. *Geophysical Journal International*, *183*(1), 407–420. doi:10.1111/j.1365-246X.2010.04743.x.

Fäh, D., Giardini, D., Bay, F., Bernardi, F., Braunmiller, J., Deichmann, N., et al. (2003). Earthquake catalog of Switzerland (ECOS) and the related macroseismic database. *Eclogae Geologicae Helvetiae—Swiss Journal of Geosciences, 96*(2), 219–236.

Fréchet, J., Thouvenot, F., Frogneux, M., Deichmann, N., & Cara, M. (2010). The M_w 4.5 Vallorcine (French Alps) earthquake of 8 September 2005 and its complex aftershock sequence. *Journal of Seismology*. doi:10.1007/s10950-010-9205-8.

Giardini, D., Wiemer, S., Fäh, D., Deichmann, N., Sellami, S., Jenni, S., & the Hazard Team of the Swiss Seismological Service, (2004). Seismic Hazard Assessment 2004. *Swiss Seismological Service*, 81.

Hitz, L., & Pfiffner, O. A. (1997). Deep seismic fan-recordings and a 3D crustal model of the eastern Aar massif. In: *Deep Structure of the Alps, Results of NRP20*, Birkhäuser, Basel, 92–100.

Husen, S., Kissling, E., Deichmann, N., Wiemer, S., Giardini, D., & Baer, M. (2003). Probabilistic earthquake location in complex three-dimensional velocity models: application to Switzerland. *Journal of Geophysical Research, 108*(B2), 2077–2096.

Kastrup, U., Deichmann, N., Fröhlich, A., & Giardini, D. (2007). Evidence for an active fault below the north-western Alpine foreland of Switzerland. *Geophysical Journal International, 169*, 1273–1288. doi:10.1111/j.1365-264X.2007.03413.x.

Kastrup, U., Zoback, M.-L., Deichmann, N., Evans, K., Giardini, D., & Michael, A. J. (2004). Stress field variations in the Swiss Alps and the northern Alpine foreland derived from inversion of fault plane solutions. *Journal of Geophysical Research, 109*, B1. doi:10.1029/2003JB002550B01402.

Kradolfer, U., & Mayer-Rosa, D. (1988). Attenuation of seismic waves in Switzerland. In: Proceedings of the XIX General Assembly of the ESC, *Recent seismological investigations in Europe* Moscow, October 1–6, 1984, 481–488.

Lomax, A., Virieux, J., Volant, P., & Thierry-Berge, C. (2000). Probabilistic earthquake location in 3D and layered models. In C. H. Thurber & N. Rabinowitz (Eds.), *Advances in Seismic Event Location* (pp. 101–134). London: Kluwer Academic Publishers.

Pavoni, N. (1977). Erdbeben im Gebiet der Schweiz. *Eclogae Geologicae Helvetiae, 70*(2), 351–370.

Pavoni, N., Maurer, H., Roth, P., & Deichmann, N. (1997). Seismicity and seismotectonics of the Swiss Alps. In: *Deep structure of the Swiss Alps, results of NRP 20*, Birkhäuser, Basel, 241–250.

Pavoni, N., & Roth, P. (1990). Seismicity and seismotectonics of the Swiss Alps. Results of microearthquake investigations 1983–1988. In: F. Roure, P. Heitzmann & R. Polino (Ed.), Deep structure of the Alps. *Mémoire de la Societé geologique de France*, N.S., 156, 129–134.

Roth, P., Pavoni, N., & Deichmann, N. (1992). Seismotectonics of the eastern Swiss Alps and evidence for precipitation-induced variations of seismic activity. *Tectonophysics*, *207*, 183–197.

Rüttener, E. (1995). Earthquake hazard estimation for Switzerland. *Matérials Géology Suisse, Geophysics* Nr. 29, Schweizerische Geophysikalische Kommission, ETH-Zürich, 106.

Rüttener, E., Eogozcue, J., Mayer-Rosa, D., & Mueller, S. (1996). Bayesian estimation of seismic hazard for two sites in Switzerland. *Natural Hazards, 14*, 165–178.

Sägesser, & Mayer-Rosa, (1978). Erdbebengefährdung in der Schweiz. *Schweizerische Bauzeitung 78*(7), 3–18.

Waldhauser, F., Kissling, E., Ansorge, J., & Mueller, St. (1998). Three-dimensional Interface Modeling with two-dimensional Seismic Data: the Alpine Crust-Mantle boundary. *Geophysical Journal International*, *135*, 264–278.

Wiemer, S., Giardini, D., Fäh, D., Deichmann, N., & Sellami, S. (2009). Probabilistic seismic hazard assessment of Switzerland: best estimates and uncertainties. *Journal of Seismology, 13*, 449–478. doi:10.1007/s10950-008-9138-7.